Structural Engineering and Mechanics, *Vol. 56, No. 3 (2015) 423-442*
DOI: http://dx.doi.org/10.12989/sem.2015.56.3.423

High-order, closely-spaced modal parameter estimation using wavelet analysis

Thai-Hoa Le[*1,2] and Luca Caracoglia[1a]

[1]*Department of Civil and Environmental Engineering, Northeastern University, 360 Huntington Ave., Boston, MA 02115, USA*
[2]*Department of Engineering Mechanics and Automation, Vietnam National University, Hanoi, 144 Xuanthuy Rd., Caugiay Dist., Hanoi, Vietnam*

(Received April 10, 2015, Revised September 7, 2015, Accepted October 20, 2015)

Abstract. This study examines the wavelet transform for output-only system identification of ambient excited engineering structures with emphasis on its utilization for modal parameter estimation of high-order and closely-spaced modes. Sophisticated time-frequency resolution analysis has been carried out by employing the modified complex Morlet wavelet function for better adaption and flexibility of the time-frequency resolution to extract two closely-spaced frequencies. Furthermore, bandwidth refinement techniques such as a bandwidth resolution adaptation, a broadband filtering technique and a narrowband filtering one have been proposed in the study for the special treatments of high-order and closely-spaced modal parameter estimation. Ambient responses of a 5-story steel frame building have been used in the numerical example, using the proposed bandwidth refinement techniques, for estimating the modal parameters of the high-order and closely-spaced modes. The first five natural frequencies and damping ratios of the structure have been estimated; furthermore, the comparison among the various proposed bandwidth refinement techniques has also been examined.

Keywords: output-only system identification; modal parameter estimation; wavelet transform; high-order and closely-spaced modes; steel building; time-frequency resolution analysis; narrowband filtering; broadband filtering

1. Introduction

Modal parameter estimation (e.g., natural frequencies, damping and mode shapes) from measured vibration responses is very important for the purpose of damage detection, model updating, structural control and dynamic assessment of engineering structures. A number of mathematical models, using output-only system identification methods, have been studied and have evolved into either parametric methods in the time domain or nonparametric methods in the frequency domain. The time-domain parametric methods, such as the Ibrahim time domain method, the eigensystem realization algorithm or the random decrement technique are preferable

*Corresponding author, Visiting Assistant Professor, E-mail: hoa.le@neu.edu
[a]Associate Professor, E-mail: lucac@coe.neu.edu

http://www.techno-press.org/?journal=sem&subpage=8 ISSN: 1225-4568 (Print), 1598-6217 (Online)

for estimating modal damping, while the frequency-domain nonparametric methods, such as the "peak-picking" and the frequency domain decomposition are preferable for estimating natural frequencies and mode shapes. Since the wavelet transform was proposed in the context of the time-frequency analysis (Daubechies 1988), it has been employed for many applications and engineering computations due to the unique capacity of analyzing arbitrary signals simultaneously on the time-frequency plane. An advantage of the wavelet transform is to analyze arbitrary signals, from linear and stationary to nonlinear, transient and non-stationary signals. Some authors pioneered the use of the wavelet transform for output-only system identification of engineering structures (e.g., Staszewski 1997, Ruzzene *et al*. 1997). The wavelet transform was considered to analyze the measured responses on the time-frequency plane, in which the natural frequencies and the damping ratios can be extracted simultaneously from the time-frequency representation of the measured responses in the frequency domain and the time domain. The wavelet transform has been used for output-only system identification of simplified mechanical systems and engineering structures (e.g., Ladies and Gouttebroze 2002, Slavic *et al*. 2003, Kijewski and Kareem 2003, Meo *et al*. 2007). The wavelet transform has its own advantages in the output-only system identification of structures owing to the simultaneous representation of the measured response on the time-frequency plane. However, computation of the wavelet transform is a complex and time-consuming task, due to the following aspects: normalization in scale, smoothing in time and scale, time-frequency resolution analysis and so on. Wavelet analysis of vibration response data on the time-frequency plane also includes need for large computer data storage and redundancy of processing information. In the wavelet analysis, nevertheless, there is a trade-off between the frequency resolution and the time resolution; a fine frequency resolution corresponds to a coarse time resolution, and conversely. Thus, the time-frequency resolution analysis becomes an important practical issue for the wavelet transform-based system identification of engineering structures. Recent applications of the wavelet transform for output-only system identification of structures have been limited to the following theoretical and practical cases: (i) simple structures and simulated experimental response data with low damping and low level of noise (e.g., Staszewski 1997, Ruzzene *et al*. 1997, Ladies and Gouttebroze 2002, Peng *et al*. 2005), (ii) few low-order fundamental modes with clear and dominant power spectra (e.g., Slavic *et al*. 2003, Chen *et al*. 2008), and (iii) well-separated natural frequencies (e.g., Meo *et al*. 2007). Utilization of the wavelet transform for the modal parameter extraction with a focus on both high-order modes and closely-spaced ones has been investigated only to a limited extent (e.g., Tan *et al*. 2007, Caracoglia and Velazquez 2008).

One of the most challenging issues in any output-only system identification method, including the wavelet transform, is to estimate the modal parameters of high-order, low-energy and closely-spaced modes of practical engineering structures. Many factors such as the influence of external excitation and noises, the resolution analysis, the low level of energy, frequency filters, and mutual interference between two closely-spaced frequencies considerably affect the accuracy in the modal parameter estimation. Furthermore, smoothing operation of the wavelet analysis on the time-frequency plane impairs the estimation of high-order frequencies and closely-spaced ones. Therefore, refinement techniques and a sophisticated time-frequency resolution analysis should be applied to enable high-order system and closely-spaced frequency identification. So far, real or traditional complex Morlet wavelets have been preferably employed for the modal identification. However, the traditional complex Morlet wavelet with only a central frequency parameter does not satisfactorily deal with the time-frequency resolution analysis in such special cases. Replacing the traditional complex Morlet wavelets with modified complex Morlet wavelets has been proposed in some applications to provide a better adaptation and flexibility for the time-frequency resolution analysis (Yan *et al*. 2006). Moreover, similar to other output-only system identification methods in both time domain and frequency domain, the wavelet transform-based modal parameter estimation becomes a more difficult task with real ambient vibration data of full-scale engineering structures. Estimated modal parameters (especially for the damping ratios) are often considerably influenced by the effects of high-frequency noise, hypothesis on external "white noise" excitation, interference of the adjacent modes and so on (e.g., Ruzzene *et al*. 1997). Extraction of free-decay functions is usually preferable in the estimation of the modal parameters to reduce noise effects, the external excitations and the cross modal interference from the measured responses. Several refinement techniques, such as random decrement technique (e.g., Slavic *et al*. 2003, Kijewski and Kareem 2003, Yan *et al*. 2006, Meo *et al*. 2006), empirical mode decomposition (e.g., Peng *et al*. 2006), filtering (e.g., Meo *et al*. 2006), pattern search (e.g., Tan *et al*. 2008) have been applied for the purposes of estimating the free-decay functions and removing perturbation of the noise, the external excitation and the cross modal interference. These afore-mentioned techniques are applicable to high-order and well-separated modes, but they do not work for closely-spaced modes. Both the modified complex Morlet wavelet, for analyzing the time-frequency resolution analysis, and the refinement techniques, for eliminating the perturbation, should be combined together to enable wavelet transform-based modal parameter estimation of high-order and closely-spaced modes. This combination is proposed and investigated as the main objective of this study.

This study examines the wavelet transform for output-only system identification of full-scale engineering structures with emphasis on modal parameter estimation for high-order and closely-spaced modes. Sophisticated time-frequency resolution analysis has been implemented by employing the modified complex Morlet wavelet. Bandwidth refinement techniques have been proposed for the special treatment of high-order, low-energy modes and closely-spaced frequencies with the adaptive time-frequency resolution analysis. The ambient response data have been measured on a 5-story steel frame building in the numerical investigation.

2. Wavelet transform

The wavelet transform of a measured response $X(t)$ is defined as the convolution operation between response $X(t)$ and mother wavelet function $\psi_{\tau,s}(t)$ as (Daubechies 1992)

$$WTC_{\psi}^{X}(\tau,s)=\int_{-\infty}^{\infty}X(t)\psi_{\tau,s}^{*}(t)dt, \tag{1}$$

where $WTC_{\psi}^{X}(s,\tau)$ is wavelet transform coefficient (WTC) at translation τ and scale s in the time-scale plane; the asterisk (*) denotes complex conjugate operator; $\psi_{\tau,s}(t)$ is the dilated and translated wavelet function at the translation τ and the scale s, derived from the "mother" wavelet function $\psi(t)$ as

$$\psi_{\tau,s}(t)=\frac{1}{\sqrt{s}}\psi\left(\frac{t-\tau}{s}\right). \tag{2}$$

Due to the two fundamental parameters (translation τ and scale s) the wavelet transforms and the wavelet transform-based quantities can represent any signal simultaneously on the time-scale (frequency) plane. The mother wavelet function, designated as the "wavelet" for the sake of brevity in the remainder of this study, satisfies the following conditions, which include an oscillatory behavior with fast decay toward zero, zero mean value, normalization and admissibility conditions

$$\int_{-\infty}^{\infty}\psi(t)dt = 0;\ \int_{-\infty}^{\infty}|\psi(t)|^2\ dt = 1;\ 0 < C_\psi = \int_{-\infty}^{\infty}\frac{|\hat{\psi}(f)|^2}{f}df < \infty, \tag{3}$$

where C_ψ is the admissibility constant, $\hat{\psi}(f)$ is the Fourier transform of $\psi(t)$ and f denotes the frequency variable. The inverse of the wavelet transform is obtained as (e.g., Daubechies 1992)

$$X(t) = \frac{1}{C_\psi}\int_{-\infty}^{\infty}\int_{-\infty}^{\infty}\frac{1}{s^2}WTC_\psi^X(\tau,s)\psi_{\tau,s}^*(t)dsd\tau\,. \tag{4}$$

The wavelet transform coefficients can be interpreted as a correlation coefficient and a measure of similitude between the wavelet and the original signal on the time-frequency plane.

3. Normalization, smoothing and ending effect treatment for wavelet transform

Normalization in the scale (frequency domain) is needed for the accuracy in the estimation of the WTC. The purpose of the normalization is to ensure that the wavelet transforms of the analytic signal at each scale are comparable to the equivalent quantitates at other scales or for other signals, while the smoothing operation aims to obtain enhanced computing accuracy by removing noise and to convert the computational domain from a local WTC to a global WTC. Each value of the $WTC_\psi^X(s,\tau)$ is normalized by a factor $1/\sqrt{s}$ on the whole scale domain (e.g., Daubechies 1998). Smoothing in both time and scale axes is important for estimating the wavelet transform-based quantities (e.g., wavelet auto spectra, wavelet cross spectra, wavelet coherence and wavelet phase difference). In the time-domain smoothing, the computed WTC is linearly averaged over a certain time segment, designated through the "time-shift" index i, or over the entire duration of the signal as (Torrence and Compo 1998)

$$< WTC_i^2(s) >= (1/i_0)\sum\nolimits_{i=i_1}^{i_2}\left|WTC_i(s)\right|^2, \tag{5a}$$

$$< WTC_i^2(s) >= (1/N)\sum\nolimits_{i=0}^{N-1}\left|WTC_i(s)\right|^2. \tag{5b}$$

In the previous equation, i is a moving index between i_1 and i_2; i_1, i_2 are the beginning time and end time of the smoothing segment; i_0 denotes the number of averaging points between i_1 and i_2, $i_0=i_2-i_1+1$; N is the number of samples on the entire time domain. In this study, the smoothing over the entire time domain in Eq. (5b) has been employed.

In the smoothing in scale, weighted scaled-averaged wavelet transform coefficients over a scale range between s_1 and s_2 have been proposed

$$< WTC_i^2(s) >= (\delta_j\delta_t / C_\delta)\sum\nolimits_{j=j_1}^{j_2}\left(\left|WTC_i(s_j)^2 / s_j\right|\right) \tag{6}$$

where j is a scale index between j_1 and j_2; δ_t is the time interval; δ_j is a scale interval; C_δ is an empirical reconstruction factor of the Morlet wavelet. The empirical factor C_δ is defined

(Torrence and Compo, 1998) as $C_\delta = (\delta_j \delta_t^{1/2} / \psi_0(0)) \sum_{j=0}^{j} \mathrm{Re}[W_\delta(s_j)] s_j^{1/2}$, in which $\psi_0(0)$ is the Morlet wavelet at the initial time t=0; $W_\delta(s_j)$ is the WTC of the delta function δ; *Re* denotes real part of the operator. Further information on the time-scale smoothing is available in Torrence and Compo (1998).

Because the wavelet function with the finite window width is applied to a finite-duration random process, loss of accuracy will occur at the beginning and the end of the time interval in the wavelet transform coefficients. This is an end effect or a cone of influence of the wavelet transform. The cone of influence depends on the scale (the frequency); concretely, the cone of influence is larger at low frequency and smaller at high frequency. A way to reduce the end effects of the wavelet spectrum is to pad the two ends of the random process with zeroes before the wavelet spectrum is computed and then remove them afterward. In this study, a simplified treatment of the end effects has been employed by zero padding over 5-second intervals at the two ends of the numerically-estimated wavelet transform coefficients. The 5-second interval removal at the two ends does not influence the accuracy of the extracted modal parameters since the strongest energy in the measured response signals occurs much later in time (after 70 seconds in this study). More sophisticated approaches are available for eliminating the end effects of the estimated wavelet transform coefficients (e.g., Torrence and Compo 1998, Kijewski and Kareem 2002). In the case of short-duration records, careful handling of the end effects should be considered.

4. Modified complex Morlet wavelet

The standard complex Morlet wavelet so far has been predominantly applied to wavelet transform-based output-only system identification. The main reason is that the complex Morlet wavelet contains harmonic components which are similar to the properties of the Fourier transform. The complex Morlet wavelet and its Fourier transform are given as (e.g., Kijeweski and Kareem 2003)

$$\psi(t) = (2\pi)^{-1/2} \exp\left(i2\pi f_c t\right) \exp\left(-t^2/2\right), \tag{7a}$$

$$\hat{\psi}(sf) = (2\pi)^{-1/2} \exp\left(2\pi^2 \left(sf - f_c\right)^2\right), \tag{7b}$$

where $\psi(t), \hat{\psi}(sf)$: complex Morlet wavelet and its Fourier transform coefficient, f: Fourier frequency variable, f_c: wavelet central frequency. It is noted that only the central frequency f_c is the fundamental parameter of the traditional complex Morlet wavelet in Eq. (7).

The meaning of the central frequency in the complex Morlet wavelet is related to the number of waveforms in a time unit or window width of wavelet. The number of waveforms in the wavelet increases with the increment of central frequency. In the other word, the central frequency refers to the resolution of the wavelet; if the central frequency increases the resolution increases with a constant width of the window. However, there is no parameter to regulate the window width in the wavelet analysis with the standard complex Morlet wavelet. Therefore, the modified complex Morlet wavelet has been introduced in order to adapt the width of the computing window in the wavelet analysis as (Yan *et al*. 2006)

$$\psi(t) = (\pi f_b)^{-1/2} \exp(j2\pi f_c t) \exp(-t^2 / f_b), \tag{8a}$$

$$\hat{\psi}(sf) = \exp(-\pi^2 f_b (sf - f_c)^2), \tag{8b}$$

where f_b denotes bandwidth parameter, which is related to the width of wavelet window. In the Eq. (8), the central frequency f_c and the bandwidth parameter f_b are combined to determine the time-frequency resolution at certain selected frequencies.

A fixed bandwidth parameter f_b=2 is used in the traditional complex Morlet wavelet. A given time-frequency resolution of the modified Morlet wavelet in Eq. (8) is determined by a balance between the width of the wavelet window and the number of waveforms in this window. A narrow window in time has good time resolution but poor frequency resolution, while a broad window has poor time resolution but good frequency resolution.

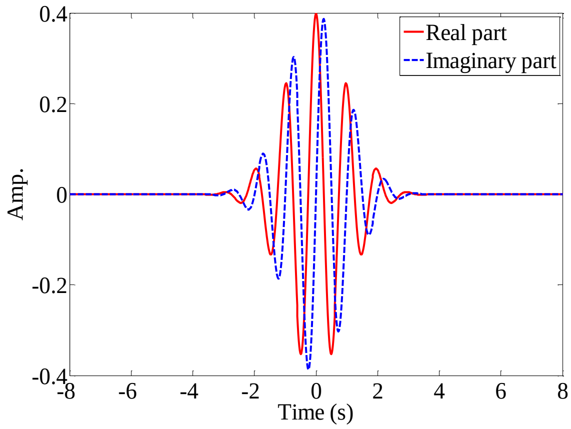

(a)

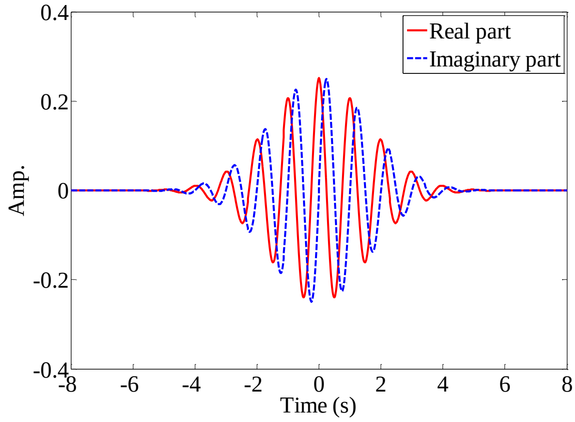

(b)

Fig. 1 Modified complex Morlet wavelets: (a) f_c=1, f_b=2; (b) f_c=1, f_b=5

Fig. 1 shows real and imaginary parts of the modified Morlet wavelet with two sets of the parameters: f_c=1 f_b=2 and f_c=1 f_b=5. These Morlet wavelets have their spectral peaks at 1Hz, which corresponds to the central frequency parameter f_c. In Fig. 1(a) the frequency of the wavelet is a unit (a waveform per time unit) and the width of window in the time domain is about [−2, 2], while in Fig. 1(b) the wavelet has unit frequency and the width of window in the time domain is [−5, 5]. If the window width is widened (larger f_b), the window amplitude must be shortened to ensure equivalent energy for the same kind of the wavelets (and inversely, see Figure 1). It is noted that $\hat{\psi}(sf)$ can be zero if f is zero, since the integral of the modified Morlet wavelet over the whole time domain is zero. This remark also results in the admissibility condition of Eq. (3) for the modified complex Morlet wavelet, which must be satisfied.

The wavelet scale is related to the Fourier frequency. The relationship between the Fourier frequency and the wavelet scale in the wavelet transform can be approximated as follows

$$f = \frac{f_c}{s}, \tag{9}$$

where s, f_c and f denote the wavelet scale, the wavelet central frequency and the Fourier frequency, respectively.

5. Modal parameters estimation

Consider a linear damped MDOF structure superimposed by N-modes; the response of the structure due to external excitation as Gaussian distributed broad-band white noises can be expressed as follows

$$X(t)=\sum_{j=1}^{N} A_i \exp(-2\pi\zeta_i f_i t)\cos(2\pi f_{di} t+\theta_i)+X_p, \tag{10}$$

where N: number of combined modes; i: index of mode; A_i: amplitude of i-th mode; θ_i: phase angle; f_i, ζ_i: undamped frequency and damping ratio of i-th mode; $f_{di}=f_i\sqrt{1-\zeta_i^2}$: damped natural frequency; X_p: perturbation due to external measurement noise or white noise (unmeasured) excitations.

No convincing study on the effect of the external excitation on the accuracy of the output-only system identification methods is available; however, a "white noise-type" external excitation is generally accepted. It is noted that some authors (e.g., Ladies and Gouttebroze 2002, Slavic *et al*. 2003, Kijewski and Kareem 2003) have used the random decrement technique (RDT) to reduce the effects of external white noise excitation, noise and cross modal interference, and to create impulse response functions of a measured structure, as damped free vibration responses, to which the wavelet transform is subsequently applied. It is argued that, however, the random decrement technique, operating as a conditional correlation function and averaging procedure, also damages high-order spectral components, which contain low energies in a practical response signal. In addition, the RDT cannot work in the case of the closely-spaced modes. Therefore, elimination of perturbation due to the measurement noise and external white noise excitation is unnecessary for the wavelet transform-based modal parameter estimation in many practical cases (e.g., Staszewski 1997). It is noted that the proposed bandwidth refinement techniques, used in this study, play a similar role to the RDT in reducing the effects of high frequency noises, white noise external excitation and cross modal interference.

Implementing the wavelet transform Eq. (1) of the theoretical response Eq. (10), one can obtain the wavelet transform coefficient as

$$WTC_\psi^X(\tau,s)=\frac{\sqrt{s}}{2}\sum_{i=1}^{N} A_i \exp(-2\pi\zeta_i f_i\tau)\,\exp(-\pi^2 f_b(sf_i-f_c)^2)\exp(j(2\pi f_{di}\tau+\theta_i)). \tag{11}$$

Because the wavelet transform coefficient is localized at a given fixed scale $s=s_i$, only the i-th mode is tuned to the wavelet scale s_i and predominantly contributes to Eq. (11), whereas the role of other modes can be negligible. Noting that from Eq. (11) one has $s_i=f_c/f_i$ or $s_i f_i-f_c=0$, the term in Eq. (11) becomes $\exp(-\pi^2 f_b(sf_i-f_c)^2)=1$. The wavelet transform coefficient at the scale s_i can be rewritten as an equivalent reduced SDOF system in the i-th mode

$$WTC_\psi^X(\tau,s_i)=\frac{\sqrt{s_i}}{2}A_i\exp(-2\pi\zeta_i f_i\tau)\exp(j(2\pi f_{di}\tau+\theta_i)). \tag{12}$$

Substituting time t for translation τ, and expressing Eq. (12) in the form of the Hilbert transform's analytic signal with instantaneous amplitude and instantaneous phase, we have

$$WTC_\psi^X(t,s_i)=B_i(t)\exp(j\varphi_i(t)), \tag{13}$$

where $B_i(t)$, $\varphi_i(t)$ denote the instantaneous amplitude and the instantaneous phase, which are determined as

$$B_i(t) = \frac{\sqrt{s_i}}{2} A_i \exp(-2\pi\zeta_i f_i t), \tag{14a}$$

$$\varphi_i(t) = 2\pi f_{di} t + \theta_i . \tag{14b}$$

Using the logarithmic expression of the instantaneous amplitude, after differentiating the logarithmic amplitude and differentiating the phase angle, one obtains

$$\frac{d \ln B_i(t)}{dt} = -2\pi\zeta_i f_i , \tag{15a}$$

$$\frac{d\varphi_i(t)}{dt} = 2\pi f_i \sqrt{1-\zeta_i^2} . \tag{15b}$$

From Eq. (15), the *i*-th natural frequency and the *i*-th damping ratio can be estimated as follows

$$f_i = \frac{1}{2\pi}\sqrt{\left(\frac{d \ln B_i(t)}{dt}\right)^2 + \left(\frac{d\varphi_i(t)}{dt}\right)^2} , \tag{16a}$$

$$\zeta_i = -\frac{1}{2\pi f_i}\frac{d \ln B_i(t)}{dt} . \tag{16b}$$

For estimating the damping ratios from the wavelet logarithmic amplitude envelope, the linear fitting technique can be applied. The afore-mentioned wavelet transform-based output-only system identification procedure has been employed for extracting the natural frequencies and the damping ratios of the ambient responses of a steel frame building with emphasis on the refinement techniques in the wavelet analysis and to detect high-order and closely-spaced modal parameters.

6. Time-frequency resolution analysis for closely-spaced frequencies

Aptitude to the multi-resolution analysis is advantageous in the wavelet transform. There is always a tradeoff between frequency resolution and time resolution. Moreover, the uncertainty principle requires that the product between the frequency resolution and the time resolution must be bounded on the time-frequency plane. The time-frequency resolution changes with the frequency and the parameters of the modified Morlet wavelet. A fine frequency resolution corresponds to a coarse time resolution, and inversely. In the processing of full-scale vibration signals, fortunately, fine frequency resolution and coarse time resolution are often employed for analyzing low frequency band. An optimal Gaussian window has been proposed in the time-frequency plane of the complex Morlet wavelet, containing the time-frequency resolution as (Ladies and Gouttebroze 2002, Kijewski and Kareem 2003)

$$\Delta f_{\psi} = \frac{1}{2\pi\sqrt{2}} , \tag{17a}$$

$$\Delta t_\psi = \frac{\sqrt{2}}{2}, \tag{17b}$$

where Δf_ψ, Δt_ψ are two reference dimensions in the frequency and the time domains. The product between the two dimensions (width and length) of the Gaussian window has the optimal value of $\Delta f_\psi \, \Delta t_\psi = 1/4\pi$; normally one has applied the relationship $\Delta f_\psi \, \Delta t_\psi \geq 1/4\pi$.

In the modified complex Morlet wavelet, the bandwidth parameter f_b or the width of the Gaussian window is added; therefore the dimensions of the Gaussian window are determined as

$$\Delta f_\psi = \frac{1}{2\pi\sqrt{f_b}}, \tag{18a}$$

$$\Delta t_\psi = \frac{\sqrt{f_b}}{2}. \tag{18b}$$

Using the inter-relation between the Fourier frequency and the wavelet central frequency, the wavelet scale, as shown in Eq. (9) with $s=f_c/f$, one obtains the time resolution and the frequency resolution from the Gaussian window as follows

$$\Delta f = \frac{\Delta f_\psi}{s} = \frac{f}{2\pi f_c \sqrt{f_b}}, \tag{19a}$$

$$\Delta t = s\Delta t_\psi = \frac{f_c\sqrt{f_b}}{2f}. \tag{19b}$$

In order to separate two closely-spaced frequencies, f_i, f_{i+1} with a difference of $\Delta f_{i,i+1}=(f_{i+1}-f_i)$ at an averaged frequency of $f_{i,i+1}=(f_{i+1}+f_i)/2$, the desired frequency resolution should be smaller than the corresponding frequency resolution, employed for the wavelet in Eq. (19); this can be determined as (Kijewski and Kareem 2003)

$$\Delta f_{i,i+1} \leq \frac{f_{i,i+1}}{2\pi f_c \sqrt{f_b}} \Big/ (2\alpha), \tag{20}$$

where $\Delta f_{i,i+1}$ is the desired frequency resolution for separating two closely-spaced frequencies f_i, f_{i+1}; α is a parameter defining overlapping of two adjacent Gaussian windows of the modified Morlet wavelet. If $\alpha=1$, the two Gaussian windows, which are centered at two closely-spaced frequencies, almost overlap. For the traditional complex Morlet wavelet, Kijewski and Kareem (2003) suggested $\alpha=2$, while Yan *et al*. (2006) used $\alpha=1.5$. However, one should not take α larger (than 2) because it can produce very coarse time resolution at very fine frequency resolution, which may influence the damping estimation. In this study, we choose $\alpha=1.5$. The central frequency and the bandwidth parameter must be selected to satisfy the following condition

$$f_c\sqrt{f_b} \geq (2\alpha)\frac{f_{i,i+1}}{2\pi\Delta f_{i,i+1}}. \tag{21}$$

As a result, one can adjust the wavelet central frequency f_c and the bandwidth parameter f_b to obtain the desired frequency resolution and the desired time resolution at a given frequency f to

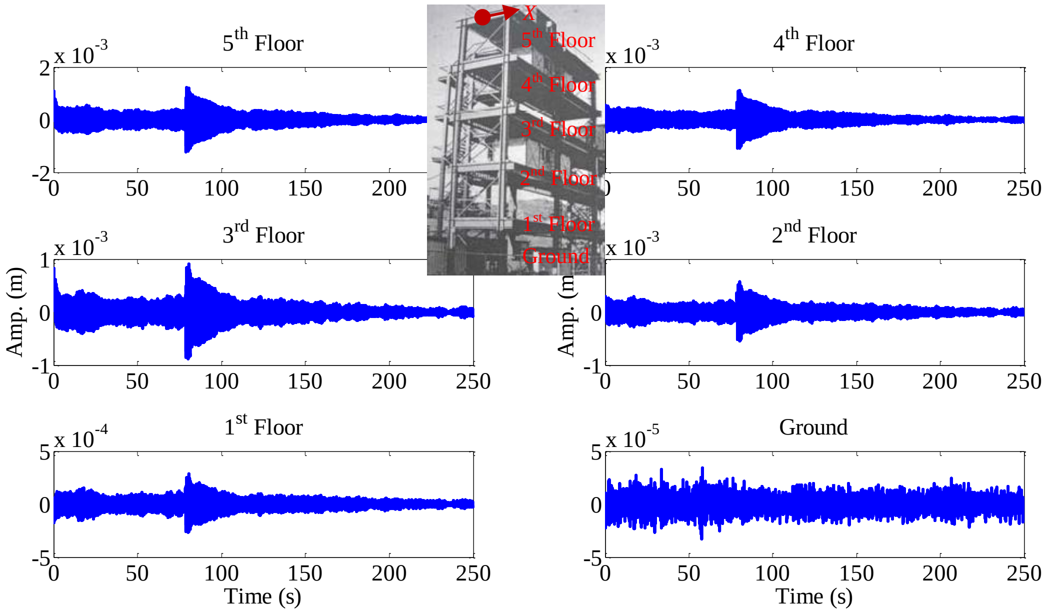

Fig. 2 Response measurements of the building at various floor levels and the ground (*X* direction)

extract high-order and closely-spaced frequencies. Furthermore, it must be noted that the selection of each set of frequency resolution and time resolution can differ at each given frequency and depends on the chosen modified Morlet wavelet function.

7. Measurements, results and discussions

Ambient vibration measurements were carried out on a 5-story steel frame building at a test site of the Disaster Prevention Research Institute (DPRI), Kyoto University (Kuroiwa and Iemura 2007). Displacement data were recorded at all 5 floor levels and ground level, over a 5-minute interval, with 100Hz sampling rate. Dual-axis displacement sensors were placed at the center of each floor. Time series of the displacement responses in the dominant *X*-direction at the five floors and ground are shown in Fig. 2.

Fig. 3(a) shows an example of power spectral density function (PSD) of the measured response on the top 5th floor at a high frequency resolution of 0.012 Hz, while 6 eigenvalues (also known as singular values) of all measured responses obtained by enhanced frequency domain decomposition (Brincker *et al*. 2001) are indicated in Fig. 3(b). In the enhanced frequency domain decomposition (EFDD), only the first eigenvalue (or the first singular value) is employed, while other higher-order eigenvalues (2nd-6th eigenvalues) can be used as a support to separate two closely-spaced frequencies or for the purpose of eliminating the perturbation of external forces and noises. However, the utilization of the higher-order eigenvalues for separating two closely-spaced frequencies is only possible for high-energy and low-order modes (Brincker *et al*. 2001), while higher-order eigenvalues cannot be used to separate closely-spaced frequencies of the high-order modes. Natural frequencies in the *X*-, *Y*-directions of the steel frame building are determined from spectral peaks observed in either the PSD of the measured response or the EFDD's first

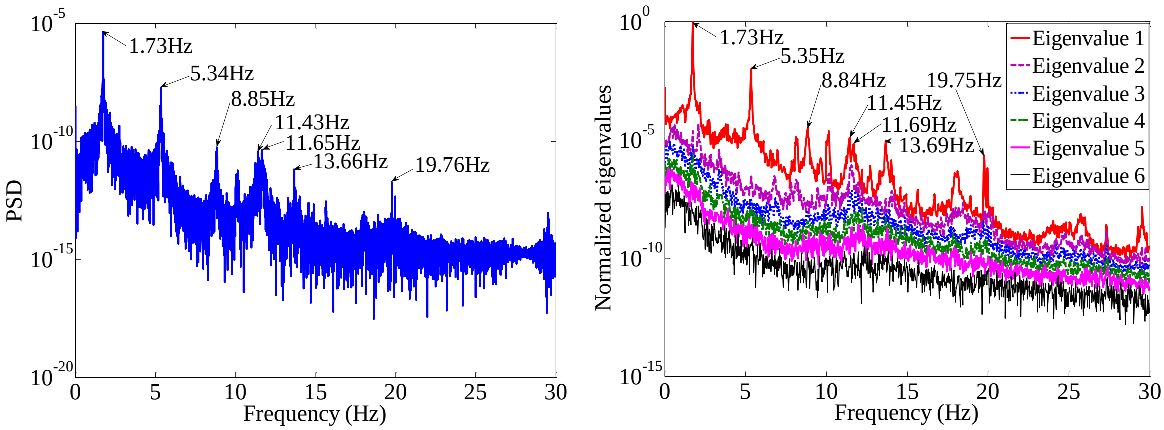

(a) (b)

Fig. 3 Natural frequency estimation of measured responses: (a) High-resolution power spectral density function (PSD), (b) enhanced frequency domain decomposition (EFDD)

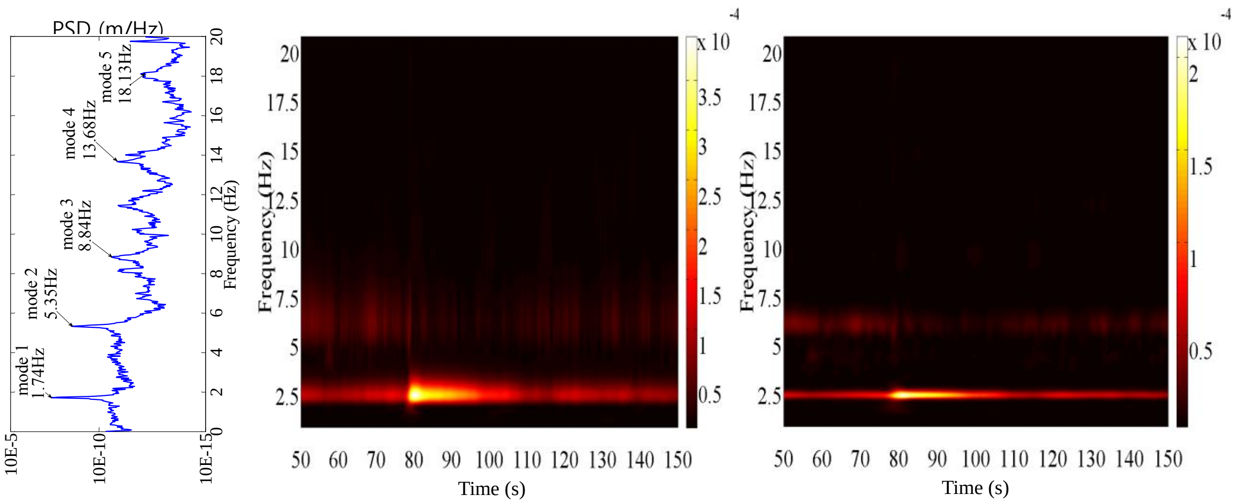

(a) (b) (c)

Fig. 4 WTC of 1st floor response: (a) PSD, (b) WTC using standard complex Morlet wavelet, (c) WTC using modified complex Morlet with f_c=2, f_b=2

eigenvalue of all measured responses. The first five structural modes in the *X*-direction only along with the order of the modes of the steel frame building were indirectly estimated by using a finite element model; they are respectively: 1.73 Hz, 5.34 Hz, 8.85 Hz, 13.66 Hz and 18.12 Hz (see Fig. 3(a)).

Wavelet analysis has been used for the measured responses. Fig. 4 shows the WTC of the measured displacement at the 1st floor in 0-20Hz frequency band between 50 s and 150 s using the standard complex Morlet wavelet (f_c=1) and the modified complex Morlet wavelet (f_c=2, f_b=2), while the PSD of the measured response is indicated in Fig. 4(a). It can be seen from the Fig. 4 that only the WTC of the 1st mode of the steel frame building can be observed, while 3rd, 4th and 5th

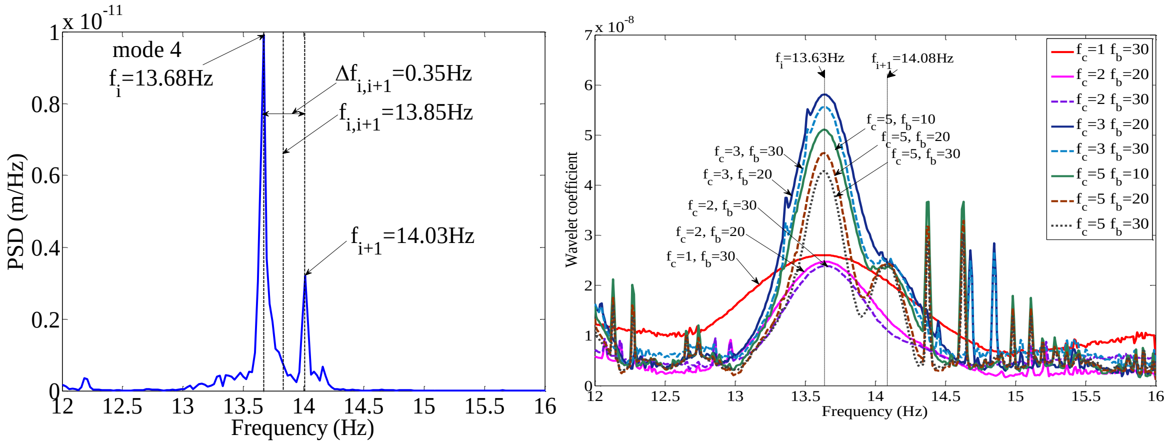

(a) (b)

Fig. 5 Time-frequency resolution analysis at closely-spaced frequencies: (a) PSD at closely-spaced frequencies, (b) resolution analysis at closely-spaced frequencies

modes are missing. The 2nd mode appears in the WTC computed by the modified complex Morlet wavelet (Fig. 4(b)), while one cannot observe this mode in the WTC using the standard complex Morlet because of a very coarse frequency resolution (Fig. 4(c)). The plausible reasons for the omission of these higher-order modes from the computed WTC are: (i) WTC of the high-order modes is small and lost as a background effect after time-scale smoothing, (ii) frequency resolution, variable over a wide frequency band between 0 and 20 Hz, is adequate for low frequency but not appropriate for higher frequency. Furthermore, two closely-spaced frequencies at 13.68 Hz and 14.03 Hz are observed in the PSD of the response (see Fig. 4(a)), while the 13.68 Hz is only discernable as the natural frequency of the 4th mode. In order to observe the higher-order modes (3rd, 4th, 5th modes) in the WTC and separate the two close frequencies at the 4th mode, special treatments of time-frequency resolution analysis and the bandwidth refinement techniques have been applied.

7.1 Treatment of closely-spaced frequencies

One aims to separate the natural frequency of the 4th mode f_i=13.68 Hz in the X direction from the adjacent frequency f_{i+1}=14.03 Hz, the natural frequency in the Y direction. Time-frequency resolution analysis is carried out using the frequency $f_{i,i+1}$=(13.68+14.03)/2=13.85 Hz as the centered frequency of the Gaussian window of the wavelets in the frequency domain, and the resolution $\Delta^* f_{i,i+1}$=(14.03−13.68)=0.35 Hz as the minimum frequency interval between two adjacent Gaussian windows of the wavelets overlapping in the frequency domain (see Fig. 5(a)). The desired frequency resolution, needed to separate two adjacent frequencies, is much lower than the resolution $\Delta^* f_{i,i+1}$=0.35 Hz. However, the desired frequency resolution is determined by Eq. (20) as $\Delta f_{i,i+1} \leq$ 0.117 Hz with α=1.5. According to Eq. (21), in order for the two Gaussian windows of two wavelets to precisely overlap at $f_{i,i+1}$=13.85Hz and $\Delta^* f_{i,i+1}$=0.35Hz, the central frequency f_c and the bandwidth parameter f_b of the modified complex Morlet wavelet must satisfy the condition $f_c \sqrt{f_b} \geq 18.9$.

Table 1 Time-frequency resolution at $f_{i,i+1}$=13.85 Hz with various pairs of central frequency f_c and bandwidth parameter f_b

f_c (Hz)	1	2		3		5		
f_b	30	20	30	20	30	10	20	30
$f_c\sqrt{f_b}$	5.4	8.9	10.9	13.4	16.4	15.8	22.3	27.3
Δf (Hz)	0.40	0.24	0.20	0.16	0.13	0.14	0.10	0.08
Δt (s)	0.20	0.33	0.40	0.49	0.60	0.57	0.80	0.98

Table 1 investigates the analyzing time and frequency resolutions at the frequency $f_{i,i+1}$=13.85 Hz, corresponding to some selected central frequency f_c and bandwidth parameter f_b of the modified Morlet wavelet. It can be seen that, if one increases the frequency resolution with the increment of both central frequency and bandwidth parameter to separate two adjacent frequencies, the time resolution accordingly decreases. However, the product between the frequency resolution and the time one is constant $\Delta f.\Delta t$=0.079. In the other words, the width (the frequency domain) and the depth of the Gaussian window of the modified Morlet wavelets are interchangeable, but the area under the Gaussian windows is the same. There is a tradeoff between fine frequency resolution and coarse time resolution. As can be seen from Table 1, only two sets of central frequency and bandwidth parameter (f_c=5 f_b=20, f_c=5 f_b=30) satisfy the conditions $f_c\sqrt{f_b}\geq 18.9$ and $\Delta f_{i,i+1}\leq 0.117$ Hz in order to completely separate the 4th modal frequency f_i=13.68 Hz (in the *X* direction) from the adjacent modal frequency f_{i+1}=14.03 Hz (in the *Y* direction).

Fig. 5(b) shows the wavelet transform coefficients in the frequency domain between 12 Hz and 16Hz, extracted from the WTC using the previously selected pairs of central frequencies and bandwidth parameters in Table 1. It is observed that one cannot separate two adjacent frequencies with the following selections of the wavelet parameters: f_c=1, f_b=30 (Δf=0.4 Hz); f_c=2, f_b=20 (Δf=0.24 Hz); f_c=2, f_b=30 (Δf=0.20 Hz); f_c=3, f_b=20 (Δf=0.16 Hz); f_c=3, f_b=30 (Δf=0.13 Hz); and f_c=5, f_b=10 (Δf=0.14 Hz). In contrast, the two adjacent frequencies begin to be well separated using the sets of parameters: f_c=5, f_b=20 (Δf=0.10 Hz); f_c=5, f_b=30 (Δf=0.08 Hz), see Table 1 and Fig. 5(b). However, the time resolutions are coarse Δt=0.8s and Δt=0.698s, respectively, in the case of the last two sets f_c=5, f_b=20 and f_c=5, f_b=30. Furthermore, the two adjacent frequencies are not being completely separated. It is suggested that one selects low central frequency f_c and high bandwidth parameter f_b in the time-frequency resolution analysis for separation of the closely-spaced frequencies. The reason for the low central frequency selection is to reduce the computational burden since the central frequency influences the number of waveforms in the Gaussian window of the wavelets. It is also advised that the proposed treatment of closely-spaced frequencies with very fine frequency resolution should be used within a given localized frequency band, which must contain the two adjacent frequencies; on the contrary, it should not be employed on the entire frequency domain to reduce the influence of the coarse time resolution on the accuracy of the modal parameter estimation.

7.2 Examination of high-order modes

In order to estimate the modal parameters of the high-order modes such as the 3rd, 4th and 5th modes in this study, we propose the bandwidth refinement treatments, which are adaptive for the

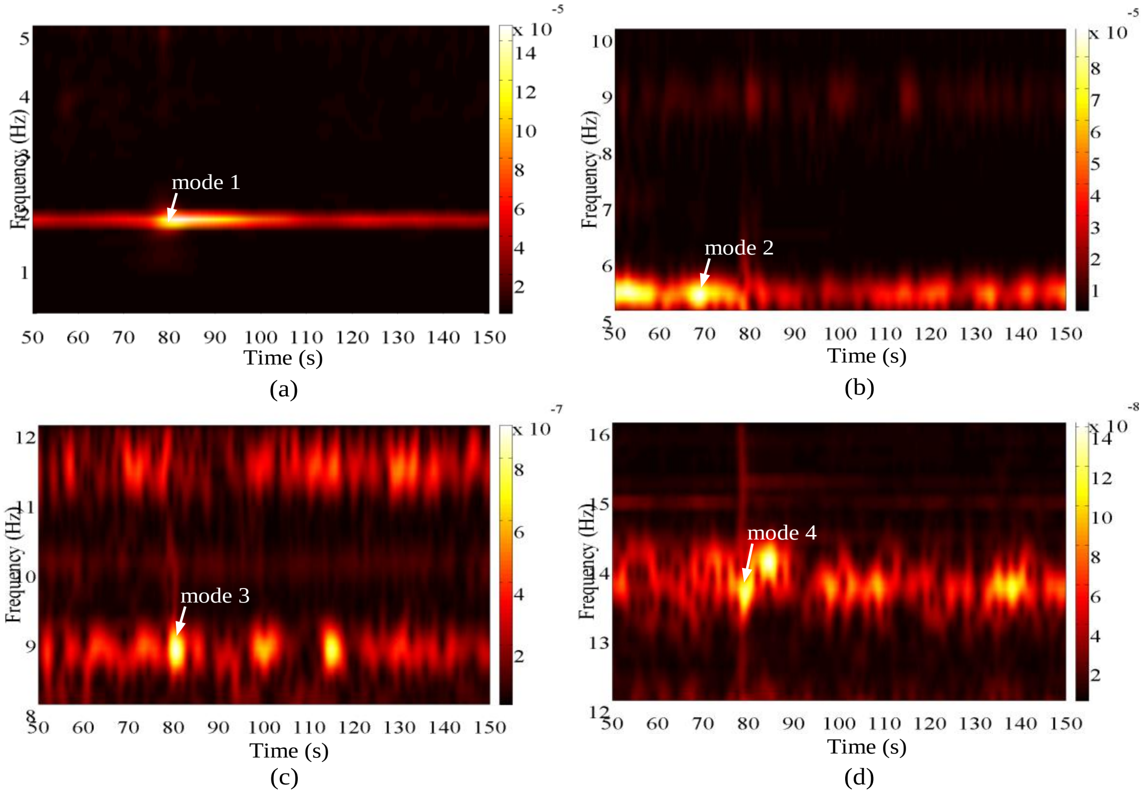

Fig. 6 WTC with bandwidth resolution adjustment: (a) bandwidth 0-5Hz (f_c=2, f_b=10), (b) bandwidth 5-10Hz (f_c=2, f_b=10), (c) bandwidth 8-12Hz (f_c=3, f_b=10), (d) bandwidth 12-16Hz (f_c=5, f_b=10)

time-frequency resolution analysis, for signal processing in a given frequency bandwidth and representation of the WTC. Possible strategies for the bandwidth refinement treatments are as follows:

(1) Bandwidth resolution adjustment: Entire frequency domain is divided into several frequency bandwidths, which contain the desired natural frequencies. The modified complex Morlet wavelet with pre-selected wavelet parameters (f_c, f_b) is applied to each frequency bandwidth. In this study, the frequency domain between 0Hz and 20Hz is segmented into the five frequency bandwidths: 0-5Hz, 5-10Hz, 8-12Hz, 12-16Hz, and 16-20Hz.

(2) Broadband filtering: measured responses are band-pass-filtered using several broad-banding bandwidths. The frequency bands containing the desired natural frequencies are maintained, while other undesired frequency bands are eliminated. The WTC is computed with each filtered broadband component at selected time-frequency resolution. Filtered broadband components 0-3Hz, 3-6Hz, 6-12Hz, and 12-24Hz of the measured responses are employed in this study.

(3) Narrowband filtering: similar to the broadband filtering treatment, the measured responses are band-pass-filtered in several narrowband components, which contain the natural frequencies. However, this narrowband filtering is localized around the identified natural frequencies. Contrary to broadband filtering, this narrowband treatment requires prior information on these natural frequencies. In this study, the measured responses are filtered at the narrowband components 1-3Hz, 4-6Hz, 8-10Hz, 13-15Hz, and 17-19Hz.

The crucial point of the proposed bandwidth refinement techniques is to divide the frequency domain of interest into several frequency bandwidths, in which different time-frequency resolutions are applied. Lower frequency resolutions are good for low frequency bands, whereas higher frequency resolutions are required for high frequency bands. These refinement techniques are employed for the modal parameter estimation of the high-order and closely-spaced modes of the 5-story steel frame building. The results are discussed in the following sub-section.

7.3 Results and discussion

Fig. 6 illustrates the WTC maps of the measured response, using the bandwidth resolution adjustment treatment with four pre-selected frequency bandwidths.

The frequency bandwidths equal to 0-5Hz, 5-10Hz, 8-12Hz, 12-16Hz, and 16-20Hz have been processed, respectively, by modified complex Morlet wavelet and using the following pairs of parameters: f_c=2, f_b=10 (Δf=0.04 Hz, Δt=1.81s); f_c=2, f_b=10 (Δf=0.13 Hz, Δt=0.59s); f_c=3 f_b=10 (Δf=0.15 Hz, Δt=0.53s); f_c=5, f_b=10 (Δf=0.13 Hz, Δt =0.57s), in which (Δf, Δt) are the resolutions determined at the corresponding natural frequencies.

Obviously, one can observe the high-order natural frequencies at selected bandwidths and resolutions (see Fig. 6); moreover, the closely-spaced frequencies can be separated in the bandwidth between 12 Hz and 16 Hz (see Fig. 6(d)). Since no filtering process is needed in the bandwidth resolution treatment, the natural frequencies and the damping ratios can be successfully extracted from the WTC maps.

In the broadband and narrowband filtering treatments, the band-pass filtering of the measured response at designed frequency bandwidths is initially required before the WTC is computed. Fig. 7(a) illustrates the time series of the broadband components from the original response computed at several frequency bandwidths, while the narrowband time series are shown in Fig. 7(b). In Fig. 7(a) the frequency bandwidths are gradually reduced by a factor of 2 from a 50 Hz-maximum frequency (due to the sampling of the signals at f_s=100 Hz), while in Fig. 7(b) the narrow frequency bandwidths are pre-selected around the identified natural frequencies.

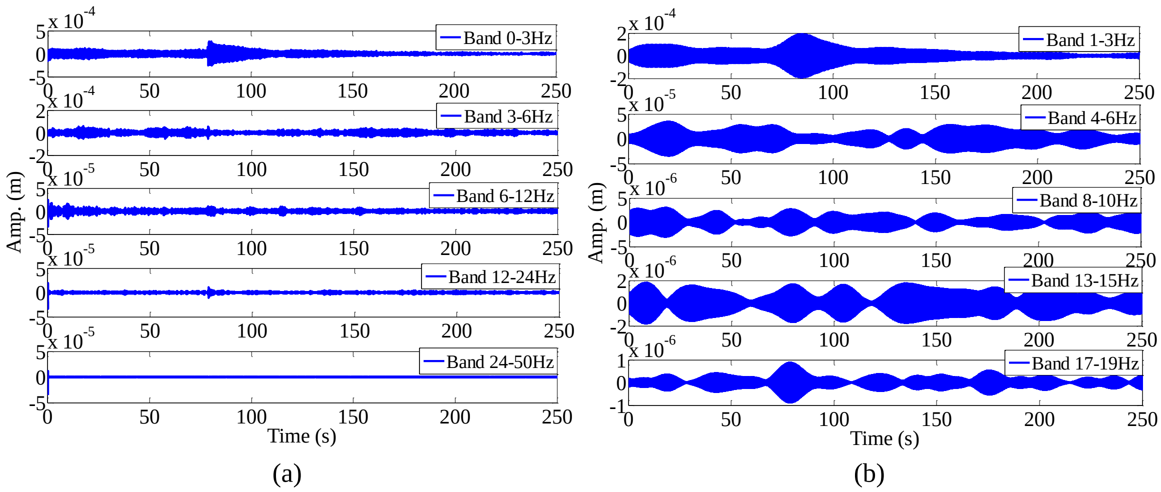

Fig. 7 Filtering components: (a) broadband components, (b) narrowband components

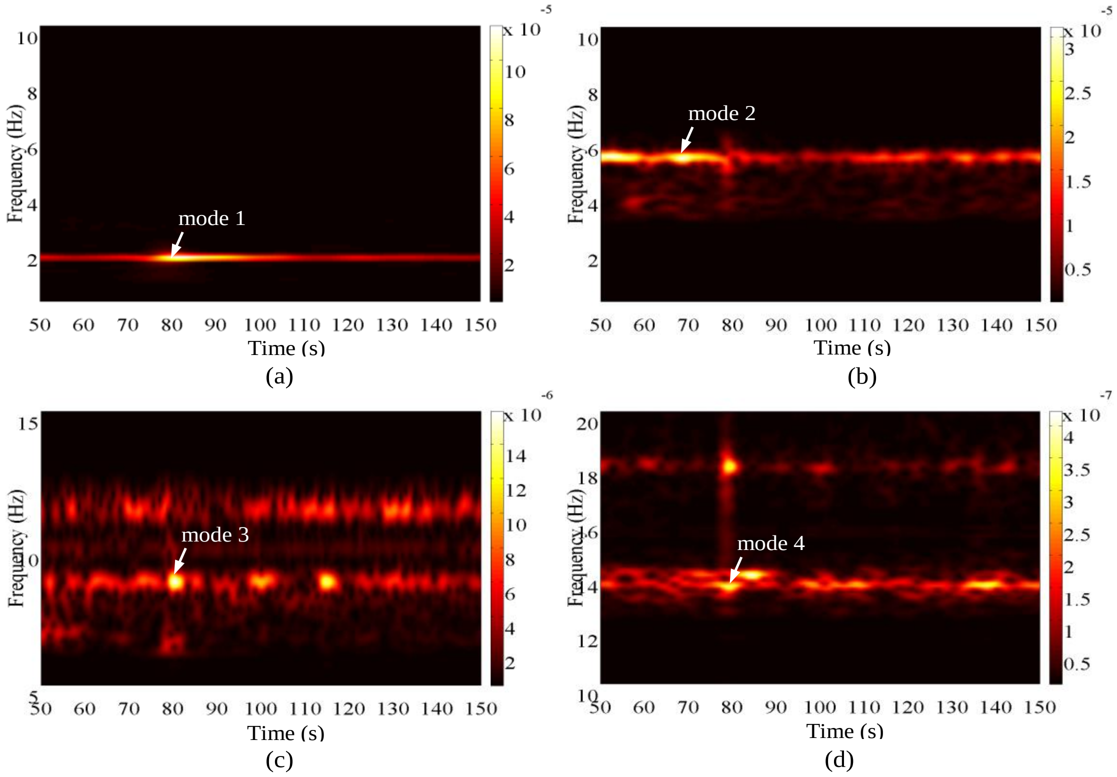

Fig. 8 WTC of broadband components: (a) bandwidth 0-3Hz (f_c=2, f_b=20), (b) bandwidth 3-6Hz (f_c=2, f_b=20), (c) bandwidth 6-12Hz (f_c=2, f_b=20), (d) bandwidth 12-24Hz (f_c=5, f_b=40)

Fig. 8 shows the WTC of the broadband components of the frequency bandwidths, respectively 0-3Hz, 3-6Hz, 6-12Hz, and 12-24Hz using the following pairs of parameters: f_c=2, f_b=20 (Δf=0.03 Hz, Δt =2.57s); f_c=2, f_b=20 (Δf=0.09 Hz, Δt =0.83s); f_c=2, f_b=20 (Δf=0.15 Hz, Δt =0.50s); and f_c=5, f_b=40(Δf=0.06 Hz, Δt =1.15s). It is noted again that frequency and time resolutions shown in parentheses (Δf, Δt) are computed at the corresponding natural frequencies. Moreover, we employ higher frequency resolutions and lower time resolutions in the WTC computations contrary to the bandwidth resolution adjustment treatment.

The natural frequencies of all the modes can be estimated; the 4th mode cannot be identified in Fig. 8(c) with the time-frequency resolution Δf=0.06 Hz, Δt =1.15s, but it is clearly observed in Fig. 8(d) with the resolution Δf=0.03 Hz, Δt=2.57s (better frequency resolution). The 5th mode is also observed at approximate frequency 18Hz in the interval 12-24 Hz, Fig. 8(d).

Fig. 9 illustrates the WTC of the narrowband components, evaluated at the frequency bandwidths 0-3 Hz, 4-6 Hz, 8-10 Hz, and 13-15 Hz and using the following pairs of parameters: f_c=2, f_b=20 (Δf=0.03 Hz, Δt =2.57s); f_c=2, f_b=20 (Δf=0.09 Hz, Δt =0.83s); f_c=2, f_b=20 (Δf=0.06 Hz, Δt =0.15s); and f_c=4, f_b=40 (Δf=0.08 Hz, Δt =0.92s). The frequency adjacent to the 4th natural frequency also is eliminated from the scalogram using the narrowband component (13-15 Hz) in Fig. 9(d). The WTC of the narrow bandwidths are visible much more clearly with the narrowband filtering treatment, since they are localized in the frequency domain but “stretched” in the time domain. This feature of the WTC is convenient for estimating the damping ratios.

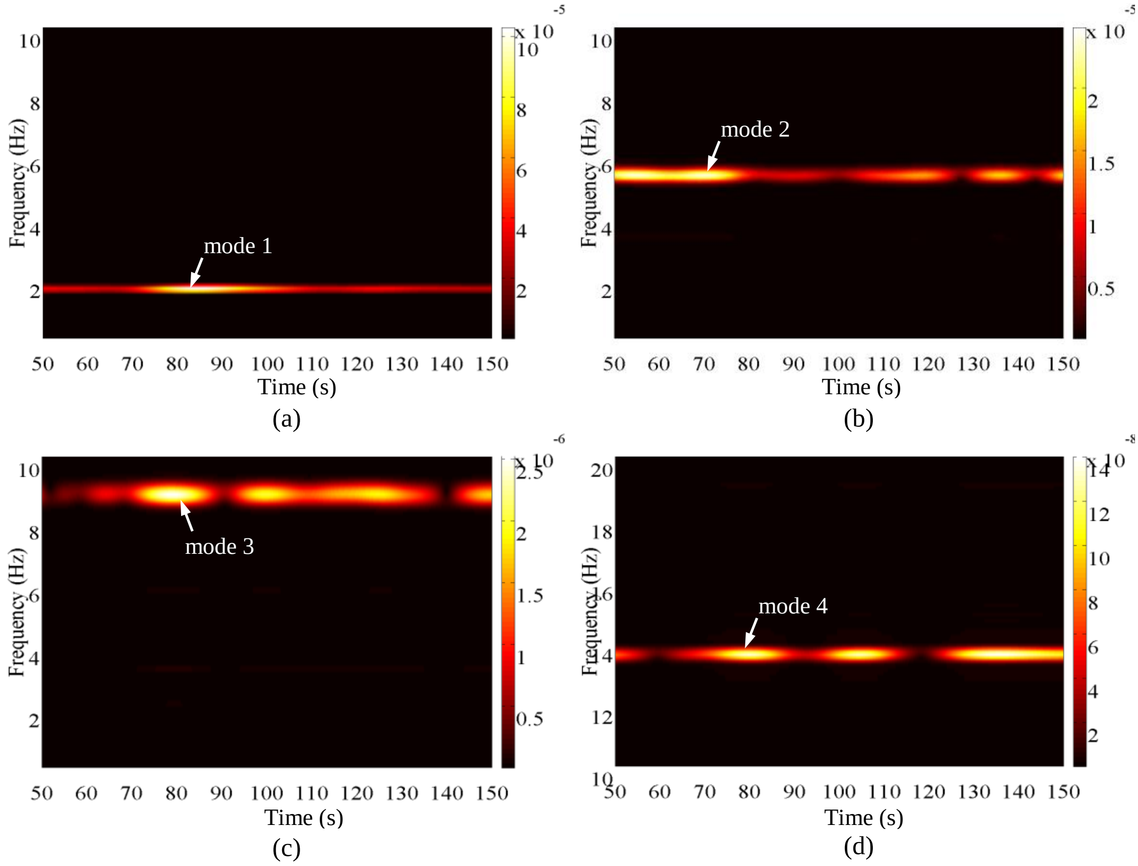

Fig. 9 WTC of narrowband components: (a) bandwidth 1-3 Hz (f_c=2, f_b=20), (b) bandwidth 4-6 Hz (f_c=2 f_b=20), (c) bandwidth 8-10 Hz (f_c=2, f_b=20), (d) bandwidth 13-15 Hz (f_c=4, f_b=40)

Fig. 10 shows the wavelet logarithmic amplitude envelopes of the WTC of the narrowband components for estimating damping of the 1st, 2nd, 3rd and 4th modes in the *X*-direction of the steel frame building. The logarithmic decrements can be estimated via linear least-squares fitting, shown as red lines in the same plots; the damping ratios are accordingly determined. The damping ratios of the first four modes are estimated as 0.52%, 1.07%, 2.07% and 1.75% in the case of the narrowband filtering treatment. Even though damping estimation has several uncertainties, one of most important aspects is to select the time window of the logarithmic amplitude envelopes adequately for damping ratio estimation. Since the Gaussian window simultaneously depends on the frequency and time resolutions, if the dimension of the frequency window is shortened to achieve fine frequency resolution, the dimension of the time window is consequently widened leading to a coarse time resolution. The selection of the time interval may significantly influence the accurate estimation of damping ratios, based on the wavelet transform. The following guidelines are proposed for modal parameter estimation using the WTC: (i) the initial time of the time window is close to the maximum value of the computed WTC at each natural frequency, (ii) short time duration is preferable for damping estimation, and (iii) a similar number of temporal cycles is employed for damping estimation at each expected natural frequency.

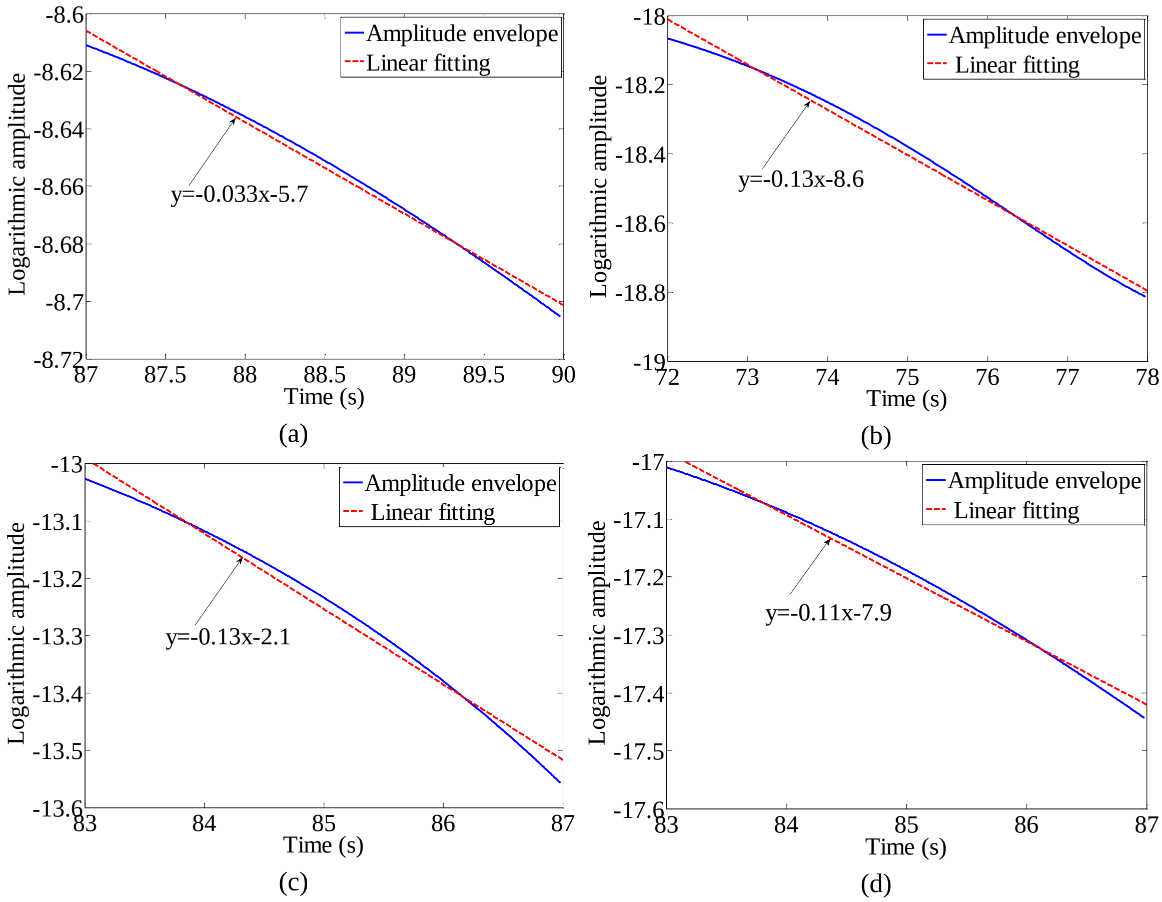

Fig. 10 Damping ratio estimation via linear fitting of WTC amplitude envelopes: (a) mode 1, (b) mode 2, (c) mode 3, (d) mode 4

Table 2 Estimated natural frequencies and damping ratios

Methods	Mode 1	Mode 2	Mode 3	Mode 4	Mode 5
	Natural frequencies (Hz)				
PSD	1.74	5.35	8.84	13.68	18.13
WT1	1.74	5.32	8.81	13.64	18.07
WT2	1.73	5.34	8.82	13.59	18.0
WT3	1.73	5.35	8.83	13.64	18.04
	Damping ratios (%)				
EFDD	0.31	0.61	1.75	1.14	0.81
WT1	0.35	1.30	2.71	2.32	2.70
WT2	0.49	0.96	1.96	2.11	2.06
WT3	0.52	1.07	2.07	1.75	1.22

Note: PSD: Power spectral density method; WT1, WT2, WT3: Respectively, wavelet transform-based bandwidth resolution adjustment, broadband filtering and narrowband filtering treatments; EFDD: enhanced frequency domain decomposition method.

The natural frequencies and damping ratios of the first five modes, estimated by using the proposed frequency bandwidth treatments (denoted as WT1, WT2 and WT3 for the sake of brevity) are listed in Table 2. The estimated values are also compared to with other output-only system identification methods, concretely the PSD for the natural frequencies and the EFDD for the damping ratios. Adequate agreement among the estimated natural frequencies is observed in the results obtained using the various refinement techniques and in comparison with other identification methods. However, a considerable difference in the estimated damping ratios can be seen. The damping ratios obtained by WT1 and WT2 (with slightly lower frequency resolution and higher time resolution) seem to be larger than the values found by WT3 (with slightly higher frequency resolution and lower time resolution). In contrast, the damping ratios determined by WT3 are closer to those predicted by EFDD. This considerable difference in the damping ratio estimation might arise from a number of sources such as filtering process, fitting operation, time-frequency resolution procedures, number of cycles, and possibly the identification methodology.

8. Conclusions

Output-only system identification of a steel frame building, using the wavelet transform with the modified complex Morlet wavelet, has been presented. The study examines several special treatments in the time-frequency analysis and the frequency bandwidth processing for the extraction of high-order and closely-spaced modal parameters. Bandwidth refinement techniques (i.e., the bandwidth resolution adjustment, the broadband filtering and the narrowband filtering) have also been investigated. Good agreement in frequency estimation and some differences in damping ratio estimation have been observed among the various identification methods. Some concluding remarks are:

(1) Modal parameters of the high-order and closely-spaced modes can be estimated well by wavelet transform if the time-frequency resolution analysis is combined with frequency bandwidth treatments.

(2) Entire frequency domain has been segmented into several smaller frequency bandwidths, in which an adaptive time-frequency resolution can be used.

(3) Time-frequency resolution analysis is an important issue for modal parameter estimation using wavelet transforms, especially for high-order and closely-spaced modes.

(4) The modified complex Morlet wavelet is advantageous for the adaptive time-frequency resolution analysis; a “low” central frequency f_c and a “high” bandwidth parameter f_b are recommended.

(5) For better estimation of damping ratios via wavelet transform the following guidelines are suggested: initial point of the amplitude envelopes at the maximum value of the WTC, short-duration amplitude envelopes with constant number of cycles.

References

Brincker, R., Ventura, C. and Andersen, P. (2001), “Damping estimation by frequency domain decomposition”, *Proceedings of International Modal Analysis Conference* (IMAC XIX), Kissimmee, USA.

Chen, S.L., Liu, J.J. and Lai, H.C. (2008), “Wavelet analysis for identification of damping ratios and natural

frequency", *Sound Vib.*, **323**, 130-147.
Caracoglia, L. and Velazquez, A. (2008), "Experimental comparison of the dynamic performance for steel, aluminum and glass-fiber-reinforced-polymer light poles", *Eng. Struct.*, **30**(4), 1113-1123.
Daubechies, I. (1992), *Ten Lectures on Wavelets*, CBMS-NSF.
Kijewski, T.L. and Kareem, A. (2003), "Wavelet transforms for system identification: considerations for civil engineering applications", *Comput. Aid. Civil Infrast. Eng.*, **18**, 341-357.
Kuroiwa, T. and Iemura, H. (2007), "Comparison of modal identification of output-only systems with simultaneous and nonsimultaneous monitoring", *Proceedings the World Forum on Smart Materials an Smart Structures Technology* (SMSST07), Chongqing & Nanjing, China.
Ladies, J. and Gouttebroze, S. (2002), "Identification of modal parameters using wavelet transform", *J. Mech. Sci.*, **44**, 2263-2283.
Meo, M., Zumpano, G., Meng, X., Cosser, E., Roberts, G. and Dodson, A. (2006), "Measurement of dynamic properties of a medium span suspension bridge by using the wavelet transform", *Mech. Syst. Signal Pr.*, **20**, 1112-1133.
Peng, Z.K., Tse, P.W. and Chu, F.L. (2005), "A comparison study of improved Hilbert-Huang transform and wavelet transform: Application to fault diagnosis for rolling bearing", *Mech. Syst. Signal Pr.*, **19**, 974-988.
Ruzzene, M., Fasana, A., Garibaldi, L. and Piombo, B. (1997), "Natural frequencies and damping identification using wavelet transform: Application to real data", *Mech. Syst. Signal Pr.*, **11**(2), 207-218.
Tan, J.B., Liu, Y., Wang, L. and Yang, W.G. (2008), "Identification of modal parameters of a system with high damping and closed spaced modes by combining continuous wavelet transform with pattern search", *Mech. Syst. Signal Pr.*, **22**, 1055-1060.
Torrence, C. and Compo, G.P. (1998), "A practical guide to wavelet analysis", *Bull. Am. Meteorol. Soc.*, **79**(1), 61-78.
Slavic, J., Simonovski, I. and Boltezar, M. (2003), "Damping identification using a continuous wavelet transform: application to real data", *J. Sound Vib.*, **262**, 291-307.
Staszewski, W.J. (1997), "Identification of damping in MDOF systems using time-scale decomposition", *Sound Vib.*, **203** (2), 283-305.
Yan, B.F., Miyamoto, A. and Bruhwiler, E. (2006), "Wavelet transform-based modal parameter identification considering uncertainty", *Sound Vib.*, **291**, 285-301.

CC